Inverse conductivity problem and the Beltrami equation

Samuli Siltanen, University of Helsinki, Finland
Applied Inverse Problems, Vienna, July 21, 2009

Finnish Centre of Excellence in Inverse Problems Research

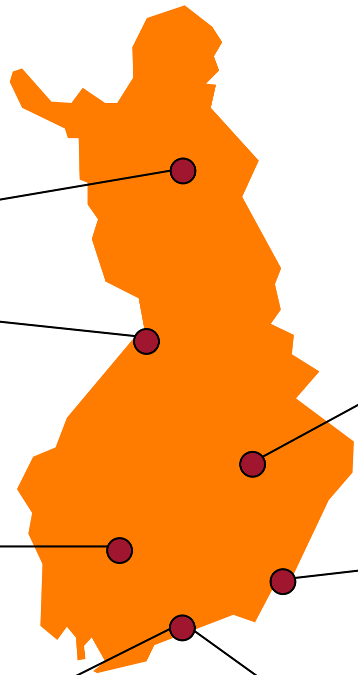

OULUN YLIOPISTO
UNIVERSITY of OULU

UNIVERSITY OF KUOPIO

TAMPERE UNIVERSITY OF TECHNOLOGY

LAPPEENRANTA UNIVERSITY OF TECHNOLOGY

TEKNILLINEN KORKEAKOULU
TEKNISKA HÖGSKOLAN
HELSINKI UNIVERSITY OF TECHNOLOGY

UNIVERSITY OF HELSINKI
Rolf Nevanlinna Institute
Research institute of mathematics, computer science and statistics

http://math.tkk.fi/inverse-coe/

This is a joint work with

Kari Astala
University of Helsinki, Finland

Jennifer Mueller
Colorado State University, USA

Lassi Päivärinta
University of Helsinki, Finland

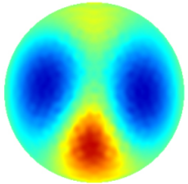

1. The inverse conductivity problem of Calderón

2. Theory of impedance imaging: infinite precision data

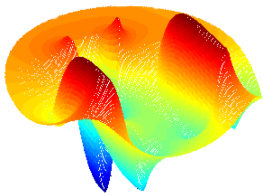

3. Computation of complex geometrical optics solutions

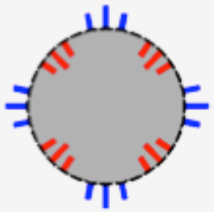

4. Simulation of measurement data

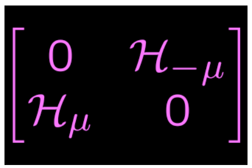

5. Numerical solution of the boundary integral equation

Electrical impedance tomography (EIT) is an emerging medical imaging method

Feed electric currents through electrodes, measure voltages

Reconstruct the image of electric conductivity in a two-dimensional slice

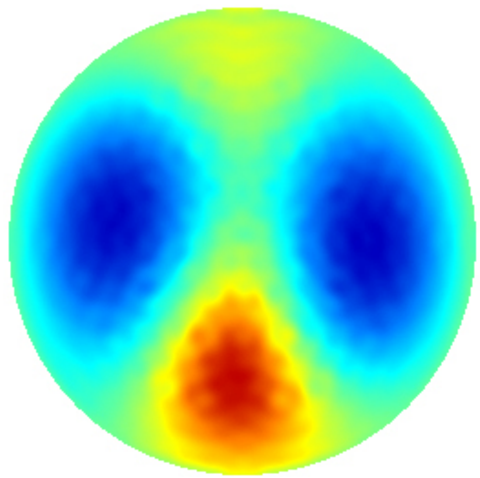

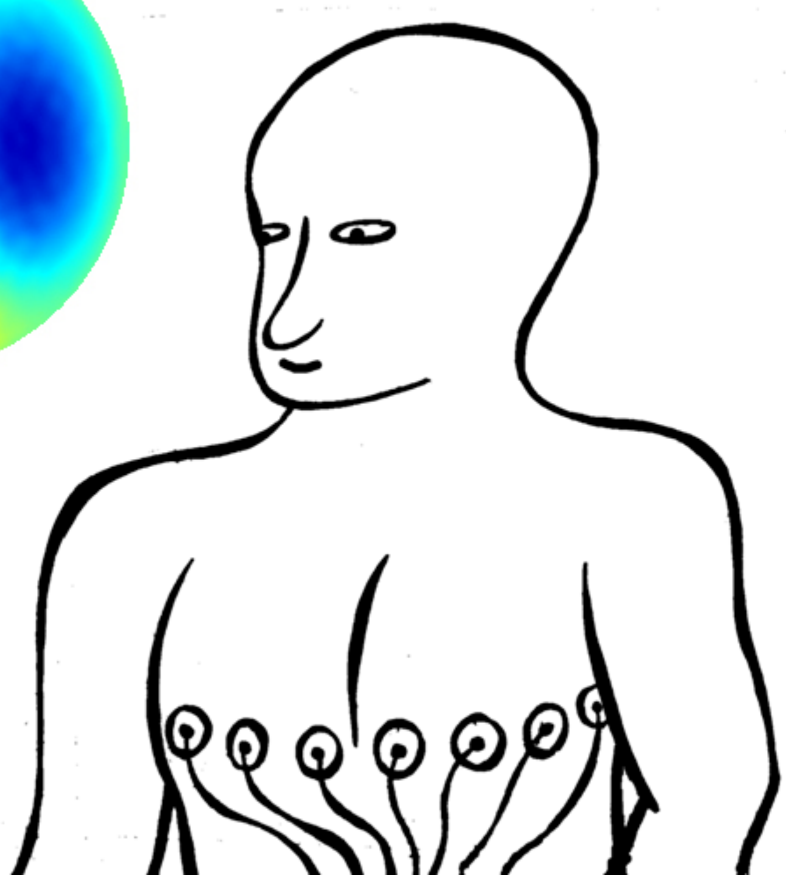

Applications include:

monitoring heart and lungs of unconscious patients, detecting pulmonary edema, enhancing ECG and EEG

The inverse conductivity problem of Calderón is the mathematical model of EIT

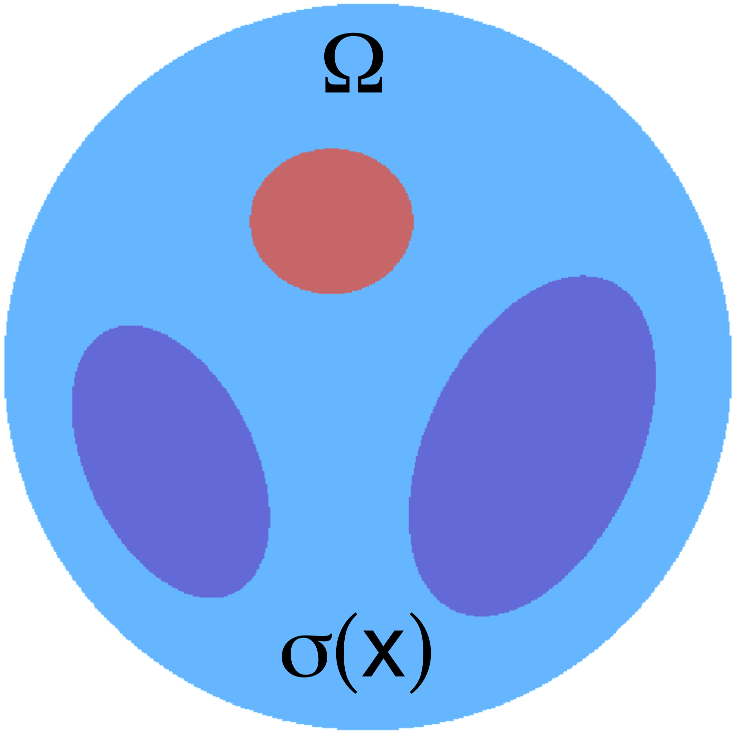

$$\Lambda_\sigma f = \sigma \frac{\partial u}{\partial \nu}\Big|_{\partial\Omega},$$

$$\begin{aligned} \nabla \cdot \sigma \nabla u &= 0 \text{ in } \Omega, \\ u|_{\partial\Omega} &= f. \end{aligned}$$

We assume that $0 < c \leq \sigma(z) \leq C$ for all $z \in \Omega$.

Problem: given the Dirichlet-to-Neumann map,
how to reconstruct the conductivity?
The reconstruction problem is nonlinear and ill-posed.

EIT reconstruction algorithms can be divided roughly into the following classes:

Linearization (Barber, Bikowski, Brown, Cheney, Isaacson, Mueller, Newell)

Iterative regularization (Dobson, Hua, Kindermann, Leitão, Lechleiter, Neubauer, Rieder, Rondi, Santosa, Tompkins, Webster , Woo)

Bayesian inversion (Fox, Kaipio, Kolehmainen, Nicholls, Somersalo, Vauhkonen, Voutilainen)

Resistor network methods (Borcea, Druskin, Vasquez)

Convexification (Beilina, Klibanov)

Layer stripping (Cheney, Isaacson, Isaacson, Somersalo)

D-bar methods (Astala, Bikowski, Bowerman, Isaacson, Kao, Knudsen, Lassas, Mueller, Murphy, Nachman, Newell, Päivärinta, Saulnier, S, Tamasan)

Teichmüller space methods (Kolehmainen, Lassas, Ola)

Methods for partial information (Alessandrini, Ammari, Bilotta, Brühl, Erhard, Gebauer, Hanke, Hyvönen, Ide, Ikehata, Isozaki, Kang, Kim, Kwon, Lechleiter, Lim, Morassi, Nakata, Potthast, Rossetand, Seo, Sheen, S, Turco, Uhlmann, Wang, and others)

This is a brief history of D-bar methods in 2D

Theory	Practice
1980 Calderón	2008 Bikowski and Mueller
1987 Sylvester and Uhlmann 1987 R G Novikov 1988 Nachman	
1996 Nachman 1997 Liu	2000 S, Mueller and Isaacson 2003 Mueller and S 2004 Isaacson, Mueller, Newell and S 2006 Isaacson, Mueller, Newell and S 2007 Murphy 2008 Knudsen, Lassas, Mueller and S
1997 Brown and Uhlmann 2001 Barceló, Barceló and Ruiz	2001 Knudsen and Tamasan 2003 Knudsen
2000 Francini	
2003 Astala and Päivärinta 2007 Barceló, Faraco and Ruiz	2008 Astala, Mueller, Päivärinta and S
2008 Clop, Faraco and Ruiz	
2008 Bukhgeim	

Reconstruction from measured data using the d-bar method based on [Nachman 1996]

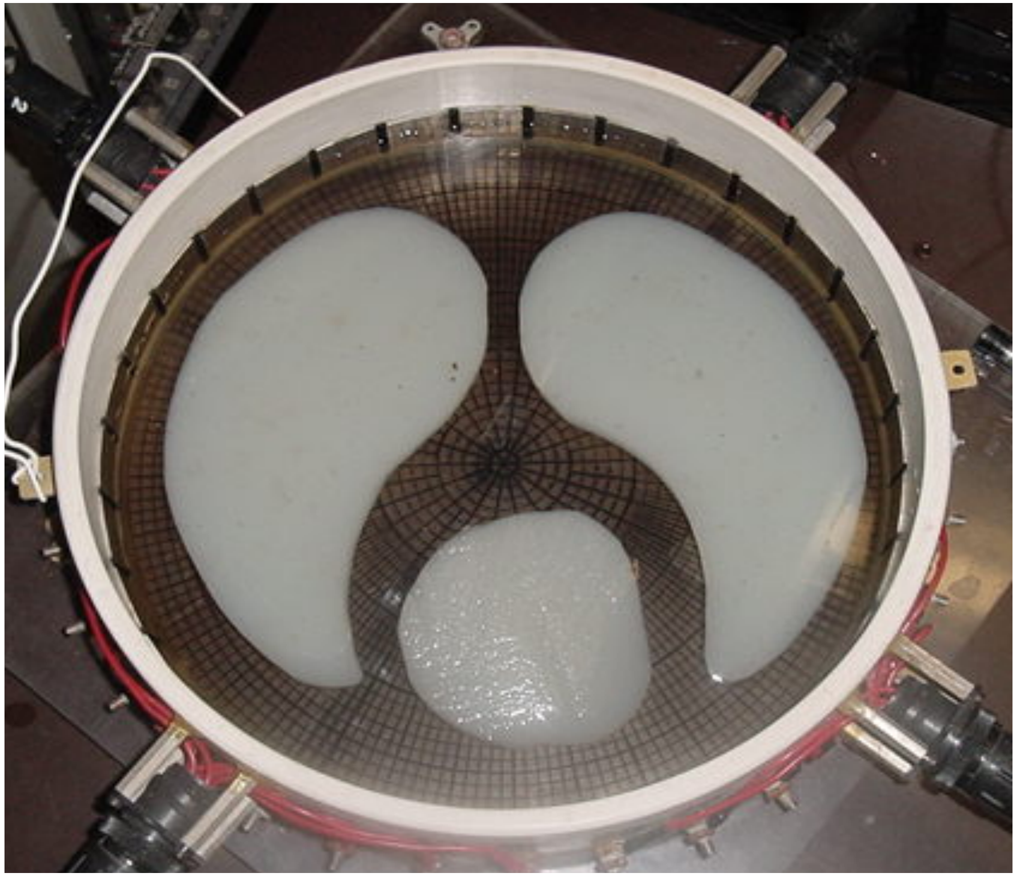

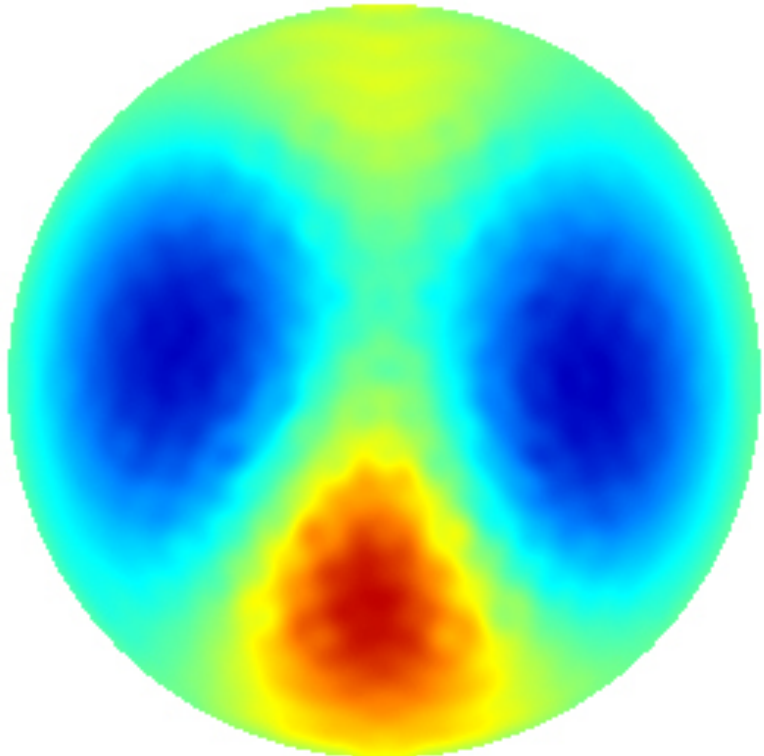

Relative error 23% (lung) and 12% (heart).
Dynamical range is 94% of the true range.

Isaacson, Mueller, Newell and S (IEEE TMI 2004)

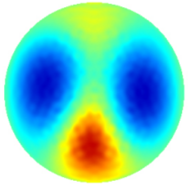

1. The inverse conductivity problem of Calderón

2. Theory of impedance imaging: infinite precision data

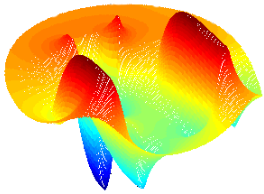

3. Computation of complex geometrical optics solutions

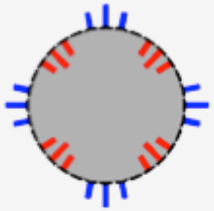

4. Simulation of measurement data

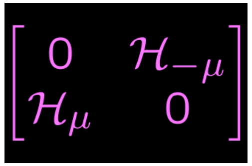

5. Numerical solution of the boundary integral equation

The reconstruction method of Astala and Päivärinta is based on complex geometrical optics solutions

Let k be a complex parameter. We define

$$\mu := \frac{1-\sigma}{1+\sigma},$$

and consider solutions $f_\mu = f_\mu(z,k)$ of the Beltrami equation

$$\boxed{\bar{\partial}_z f_\mu = \mu \overline{\partial_z f_\mu},}$$

where the solutions can be written in the form $f_\mu(z,k) = e^{ikz}(1+\omega(z,k))$ with asymptotics

$$\omega(z,k) = \mathcal{O}\left(\frac{1}{z}\right) \text{ as } |z| \to \infty$$

Reconstruction Step 1: Recover the μ-Hilbert transform from measured data

We have for real-valued functions $g : \partial\Omega \to \mathbb{R}$

$$\partial_T \mathcal{H}_\mu g = \Lambda_\sigma g,$$

where ∂_T is the tangential derivative.
The μ-Hilbert transform $\mathcal{H}_\mu$ is real-linear:

$$\mathcal{H}_\mu(ig) = i\mathcal{H}_{-\mu}(g).$$

We can find $\mathcal{H}_{-\mu}$ using $\mathcal{H}_\mu$ and the identity

$$\mathcal{H}_\mu \circ (-\mathcal{H}_{-\mu})u = (-\mathcal{H}_{-\mu}) \circ \mathcal{H}_\mu u = u - \mathcal{L}u,$$

where $\mathcal{L}\phi := |\partial\Omega|^{-1} \int_{\partial\Omega} \phi \, ds$.

Reconstruction Step 2: Solve a boundary integral equation for the traces of the CGO solutions

In analogy with the Riesz projections we define

$$\mathcal{P}_\mu g = \frac{1}{2}(I + i\mathcal{H}_\mu)g + \frac{1}{2}\mathcal{L}g.$$

Further, denote

$$\mathcal{P}_0^k := e^{-ikz}\mathcal{P}_0 e^{ikz}.$$

Then we can solve for the traces of f_μ from

$$f_\mu|_{\partial\Omega} + e^{ikz} = (P_\mu + P_0^k) f_\mu|_{\partial\Omega}.$$

Reconstruction Step 3: Find values of CGO solutions at a point outside the domain Ω

Choose $z_0 \in \mathbb{R}^2 \setminus \overline{\Omega}$. For each $k \in \mathbb{C}$, use $f_\mu|_{\partial\Omega}$ and $f_{-\mu}|_{\partial\Omega}$ to find $\omega^+|_{\partial\Omega}$ and $\omega^-|_{\partial\Omega}$ using

$$\begin{aligned} f_\mu(z,k) &= e^{ikz}(1+\omega^+(z,k)), \\ f_{-\mu}(z,k) &= e^{ikz}(1+\omega^-(z,k)). \end{aligned}$$

Now $\omega^+(z,k)$ and $\omega^-(z,k)$ are analytic and $\mathcal{O}(1/z)$ outside Ω. Thus we can compute $\omega^\pm(z_0,k)$ by an expansion $\sum_{j=1}^{\infty} c_j z^{-j}$. Define

$$\nu_{z_0}(k) = -\frac{\overline{f_\mu(z_0,k)} - \overline{f_{-\mu}(z_0,k)}}{f_\mu(z_0,k) + f_{-\mu}(z_0,k)}.$$

Reconstruction Step 4: Use the transport matrix to find values of CGO solutions inside Ω

$$
\begin{aligned}
h^+ &= (f_\mu + f_{-\mu})/2, \\
h^- &= i(\overline{f_\mu} - \overline{f_{-\mu}})/2, \\
u_1 &= h^+ - ih^-, \\
u_2 &= i(h^+ + ih^-).
\end{aligned}
$$

$$
\begin{aligned}
\alpha_\mu(z_0, k) &= a_1 + ia_2, \\
\alpha_{-\mu}(z_0, k) &= b_2 - ib_1.
\end{aligned}
$$

$$
\begin{aligned}
\bar\partial_k \alpha_\mu &= \nu_{z_0}(k)\overline{\partial_k \alpha_\mu}, \\
\bar\partial_k \alpha_{-\mu} &= -\nu_{z_0}(k)\overline{\partial_k \alpha_{-\mu}},
\end{aligned}
$$

$$
\alpha_{\pm\mu}(z, k) \sim e^{ikz}.
$$

$$
\begin{aligned}
u_1(z, k_0) &= a_1(k_0)u_1(z_0, k_0) + a_2(k_0)u_2(z_0, k_0), \\
u_2(z, k_0) &= b_1(k_0)u_1(z_0, k_0) + b_2(k_0)u_2(z_0, k_0).
\end{aligned}
$$

Final steps of reconstruction

Since we know the values of CGO solutions inside the domain, we can write

$$\mu(z) = \frac{\bar{\partial}_z f_\mu(z, k0)}{\overline{\partial_z f_\mu}(z, k0)},$$

and finally recover the conductivity as

$$\sigma(z) = \frac{1 - \mu(z)}{1 + \mu(z)}.$$

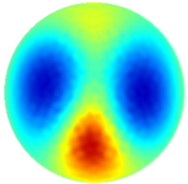

1. The inverse conductivity problem of Calderón

Λ

2. Theory of impedance imaging: infinite precision data

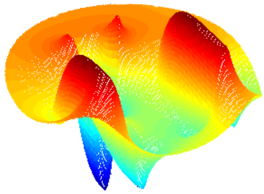

3. Computation of complex geometrical optics solutions

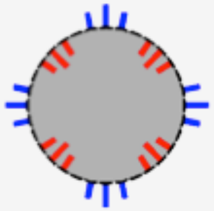

4. Simulation of measurement data

$$\begin{bmatrix} 0 & \mathcal{H}_{-\mu} \\ \mathcal{H}_{\mu} & 0 \end{bmatrix}$$

5. Numerical solution of the boundary integral equation

Construction of CGO solutions

Define the solid Cauchy transform by

$$Pf(z) = -\frac{1}{\pi}\int_{\mathbb{C}} \frac{f(\lambda)}{\lambda - z} dm(\lambda),$$

and $Sf = \partial P f$; note that $S(\bar{\partial} f) = \partial f$. Denote

$$\begin{aligned} \alpha(z,k) &= -i\overline{k}\,\mathrm{exp}(-i(kz + \overline{k}\overline{z}))\mu(z), \\ \nu(z,k) &= \mathrm{exp}(-i(kz + \overline{k}\overline{z}))\mu(z), \end{aligned}$$

and define a real-linear operator K by

$$Kg = P(I - \nu\overline{S})^{-1}(\alpha\overline{g}).$$

Then $I - K$ is invertible in $L^p(\mathbb{C})$ and equation

$$(I - K)\omega = K(\chi_\Omega)$$

has a unique solution with $\omega(z,k) = \mathcal{O}(1/z)$.

Numerical solution requires a finite computational domain.

To this end, we consider periodic functions.

The plane is tiled by the square S.

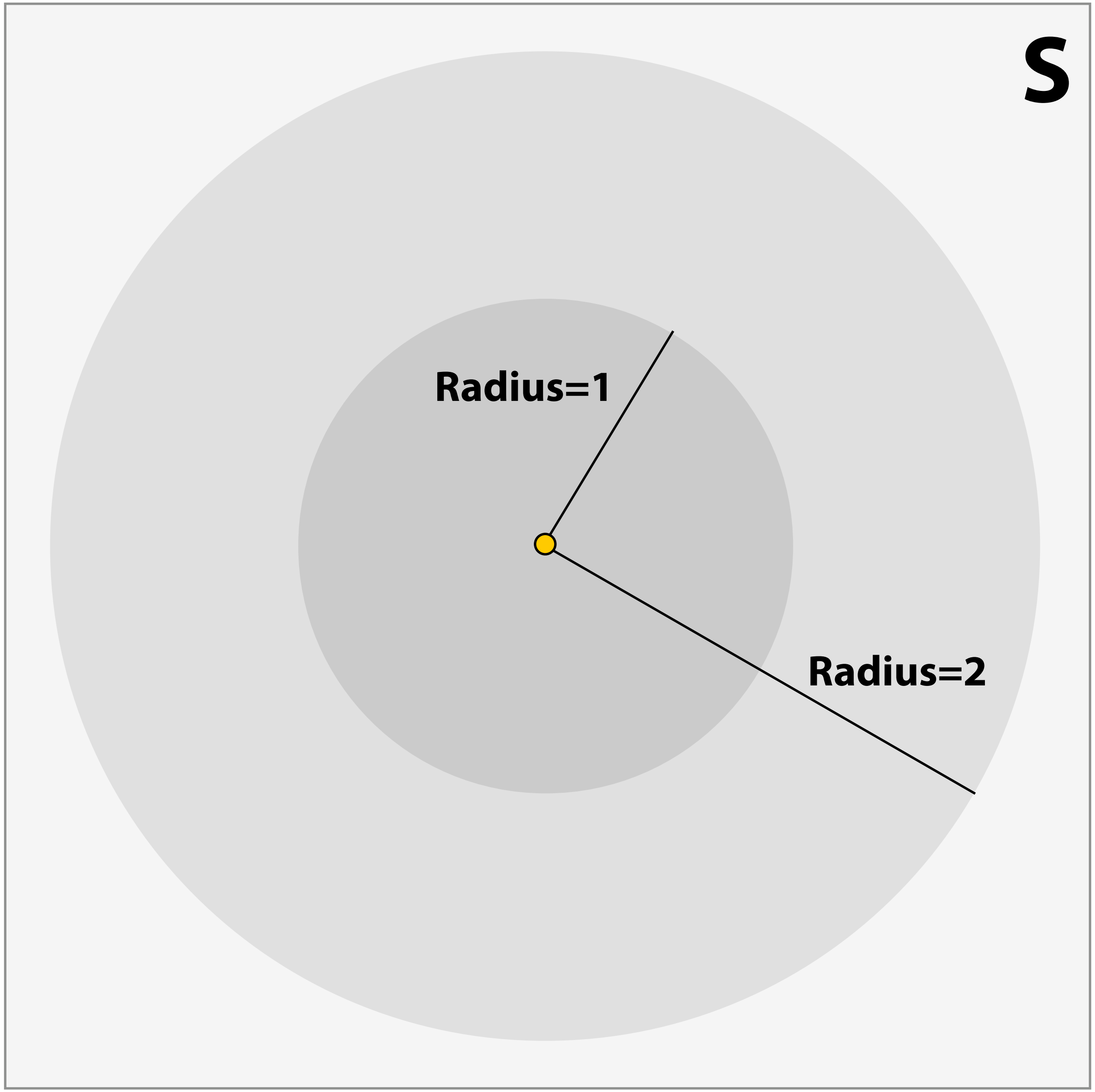

In practice, CGO solutions are computed by solving a related periodic equation numerically

Define a periodic Green function by

$$\tilde{g}(z + j2s + i\ell 2s) = \frac{\eta(z)}{\pi z}$$

and periodic approximate Cauchy transform by

$$\tilde{P}f(z) = \int_S \tilde{g}(z-w)f(w)dw,$$

Set $\rho(f) = \overline{f}$ and $\tilde{K}\varphi = \tilde{P}(I - \nu\rho\partial\tilde{P})^{-1}(\alpha\overline{\varphi})$.

Theorem 1 (Astala, Mueller, Päivärinta, S)
There exists a unique periodic solution to

$$(I - \tilde{K})\tilde{\omega} = \tilde{K}(\chi_\Omega).$$

Furthermore, $\omega(z,k) = \tilde{\omega}(z,k)$ *for* $z \in \Omega$.

We form a grid suitable for FFT (fast Fourier transform).

Here 8x8 grid is shown; in practice we typically use 512x512 points.

Periodic functions are represented by their values at the grid points.

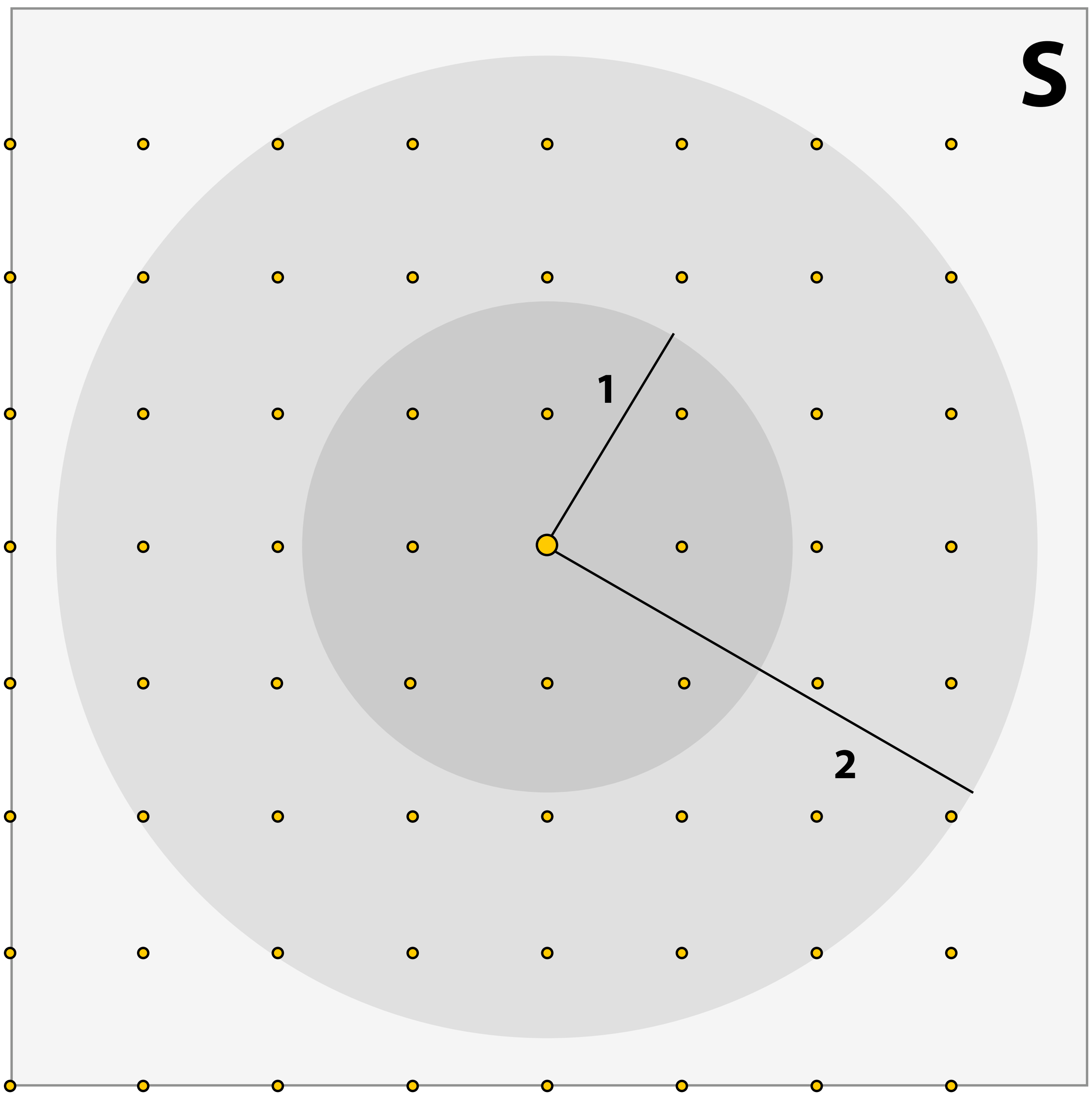

Periodic Cauchy transform is implemented using Fast Fourier Transform

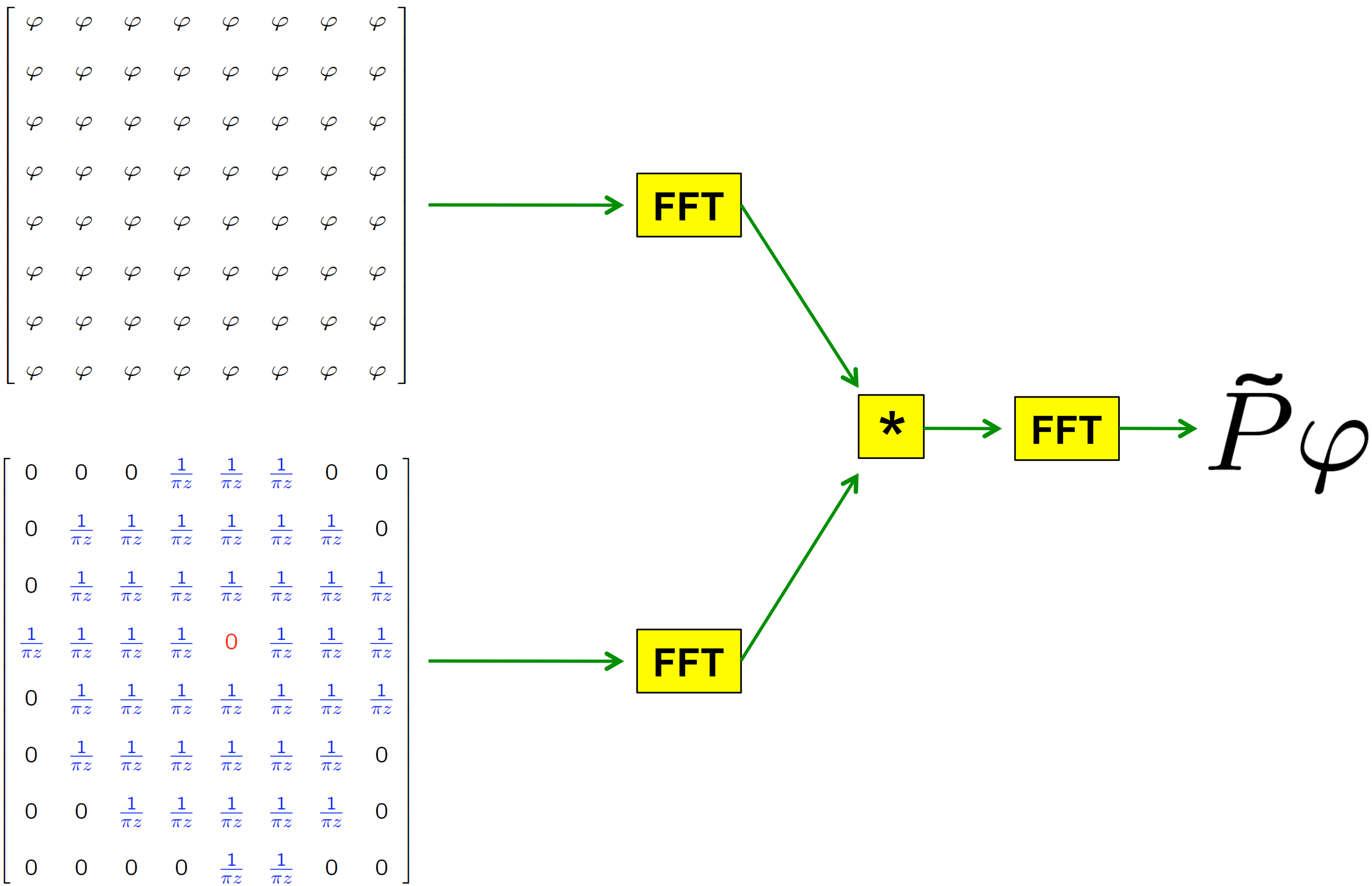

The computation of the CGO solutions is based on this theorem and on the use of GMRES

Theorem (Astala, Mueller, Päivärinta & S)
Define truncated operator

$$\tilde{K}_L(\varphi) := \tilde{P} \sum_{\ell=0}^{L} (\nu\rho\,\partial\tilde{P})^{\ell}(\alpha\overline{\varphi}).$$

Let $\varepsilon > 0$ and take any $k \in \mathbb{C}$. Then for large L there exists a unique $2s$-periodic solution to

$$(I - \tilde{K}_L)\,\tilde{\omega}_L = \tilde{K}_L(\chi_\Omega),$$

and the following estimate holds:

$$\|\tilde{\omega}(\,\cdot\,,k) - \tilde{\omega}_L(\,\cdot\,,k)\|_{L^2(Q)} \leq \varepsilon.$$

Here are examples of numerical evaluation of CGO solutions corresponding to a discontinuous σ

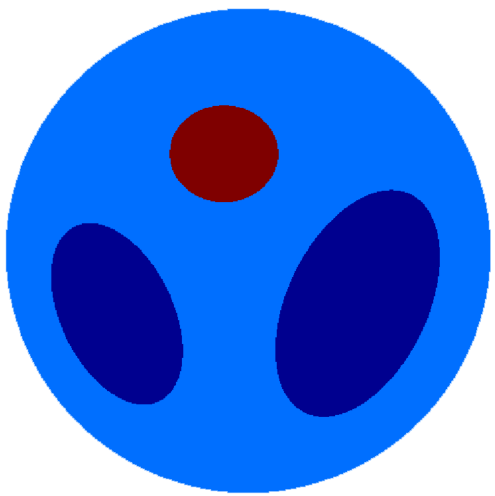

$$\mu = \frac{1-\sigma}{1+\sigma}$$

$$\bar{\partial}_z f_\mu = \mu \overline{\partial_z f_\mu}$$

$$f_\mu(z,k) = e^{ikz}(1+\omega(z,k))$$

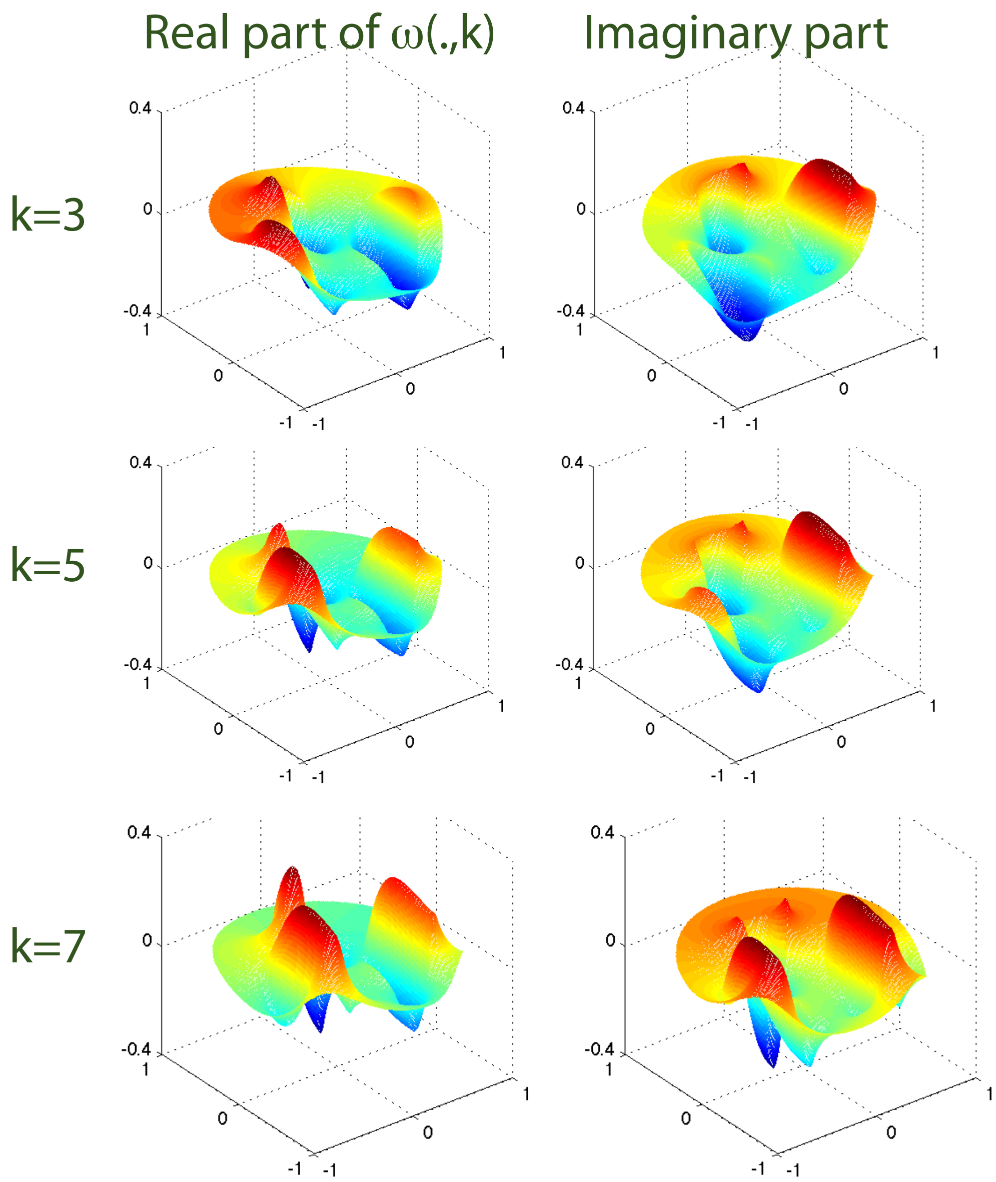

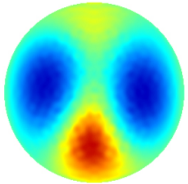

1. The inverse conductivity problem of Calderón

Λ

2. Theory of impedance imaging: infinite precision data

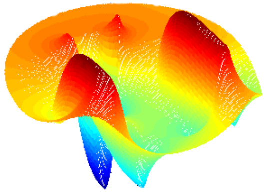

3. Computation of complex geometrical optics solutions

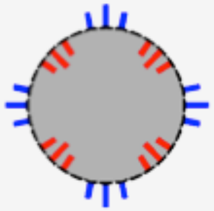

4. Simulation of measurement data

$$\begin{bmatrix} 0 & \mathcal{H}_{-\mu} \\ \mathcal{H}_{\mu} & 0 \end{bmatrix}$$

5. Numerical solution of the boundary integral equation

This is a typical configuration for electrode measurements in EIT

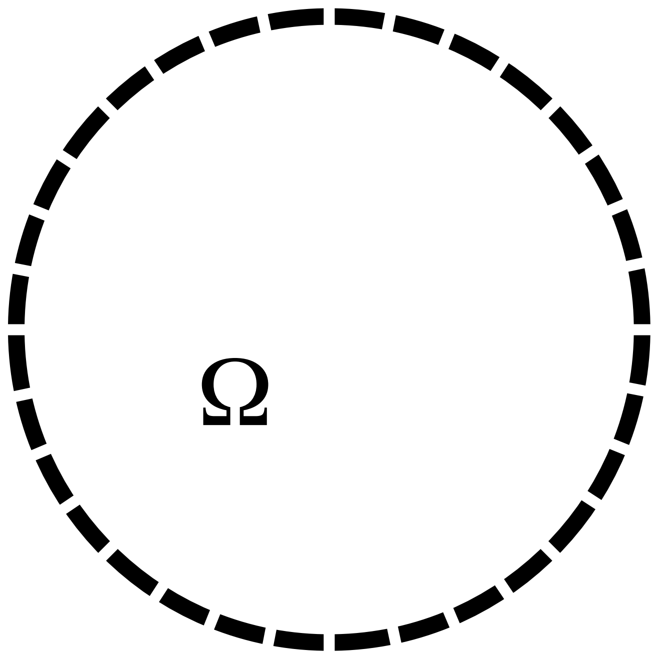

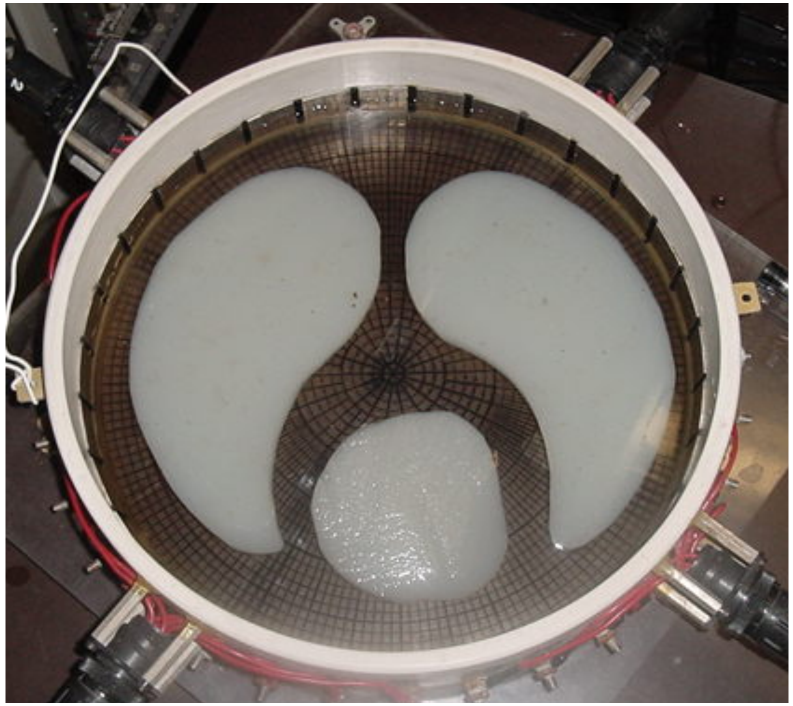

Here we have N=32 electrodes.
The machine is in Rensselaer Polytechnic Institute, USA.

We use a trigonometric basis to express functions defined at the boundary:

$$
\begin{aligned}
\phi_0(\theta) &= (\sqrt{2\pi})^{-1}, \\
\phi_1(\theta) &= (\sqrt{\pi})^{-1} \cos\theta, \\
\phi_2(\theta) &= (\sqrt{\pi})^{-1} \sin\theta, \\
\phi_3(\theta) &= (\sqrt{\pi})^{-1} \cos 2\theta, \\
\phi_4(\theta) &= (\sqrt{\pi})^{-1} \sin 2\theta, \\
\vdots \quad &\vdots \quad \vdots \\
\phi_{2N-1}(\theta) &= (\sqrt{\pi})^{-1} \cos N\theta, \\
\phi_{2N}(\theta) &= (\sqrt{\pi})^{-1} \sin N\theta.
\end{aligned}
$$

We expand real-valued functions as

$$
f(\theta) \approx \sum_{n=0}^{2N} \left(\int_0^{2\pi} f(\theta)\phi_n(\theta)\, d\theta \right) \phi_n(\theta).
$$

The trigonometric basis functions approximate discrete current patterns

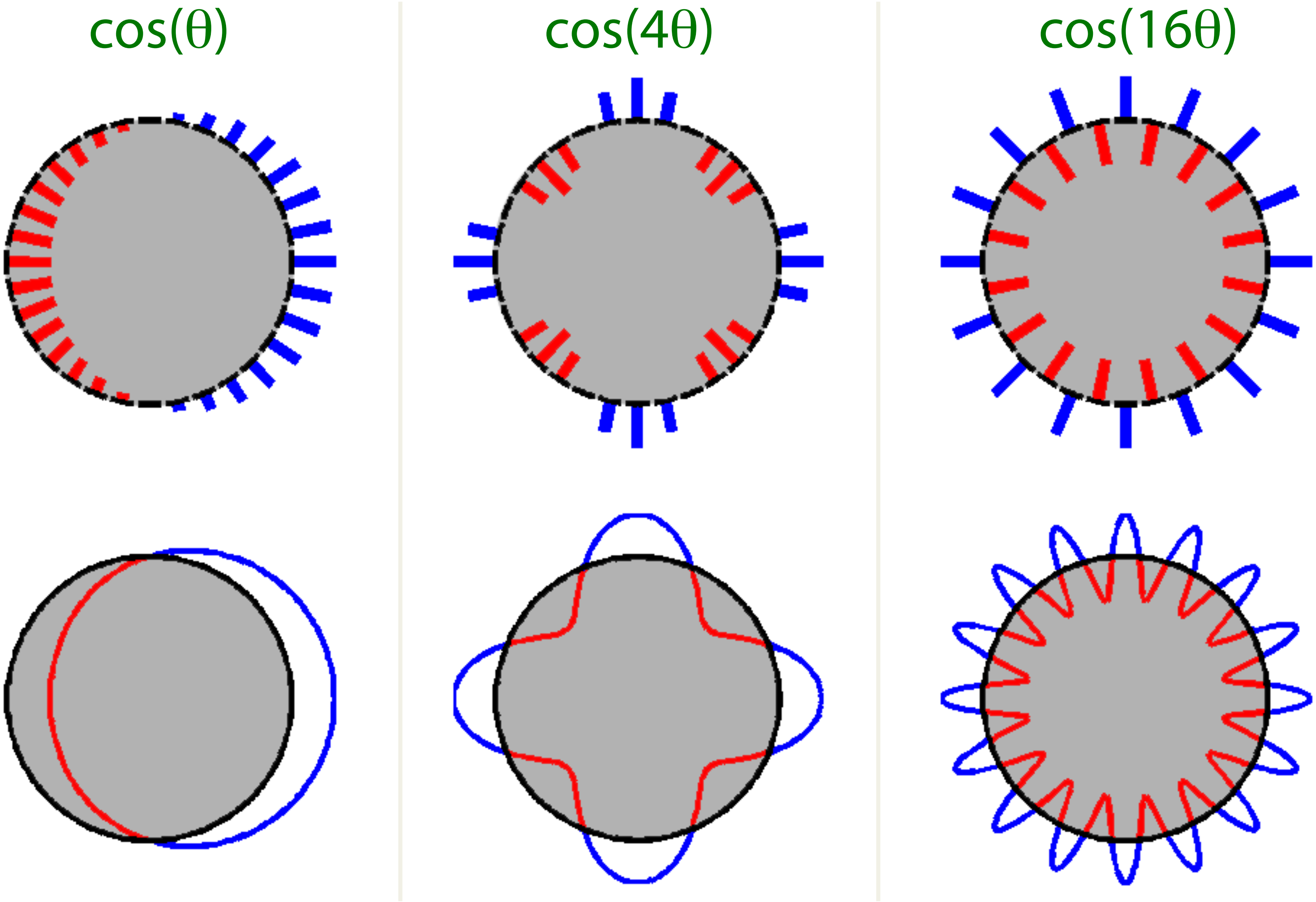

We simulate noisy data by computing the ND map, adding noise, and finding the DN map

Solve the Neumann problems

$$\nabla \cdot \sigma \nabla u^{(n)} = 0 \text{ in } \Omega, \qquad \sigma \frac{\partial u^{(n)}}{\partial \nu}\Big|_{\partial\Omega} = \phi_n,$$

with $n = 1, \ldots 2N$ and $\int_{\partial\Omega} u^{(n)} ds = 0$. Define $2N \times 2N$ Neumann-to-Dirichlet matrix R_σ by

$$R_\sigma[\ell, n] := \int_{\partial\Omega} u^{(n)} \overline{\phi_\ell}\, ds.$$

Add simulated measurement noise by

$$R_\sigma^\varepsilon := R_\sigma + cE, \qquad E[\ell, n] \sim \mathcal{N}(0, 1),$$

and approximate the DN map Λ_σ by the matrix

$$L_\sigma^\varepsilon = (R_\sigma^\varepsilon)^{-1}.$$

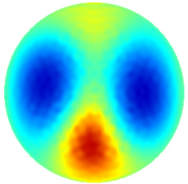

1. The inverse conductivity problem of Calderón

Λ

2. Theory of impedance imaging: infinite precision data

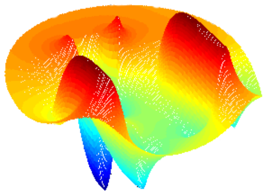

3. Computation of complex geometrical optics solutions

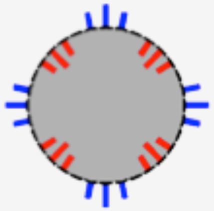

4. Simulation of measurement data

$$\begin{bmatrix} 0 & \mathcal{H}_{-\mu} \\ \mathcal{H}_{\mu} & 0 \end{bmatrix}$$

5. Numerical solution of the boundary integral equation

Numerical solution of the boundary integral equation is based on matrix pseudoinversion

We represent complex-valued functions by expanding the real and imaginary parts in the finite trigonometric basis. Then we can solve for the traces of f_μ from

$$\begin{bmatrix} \mathrm{Re}\, f_\mu|_{\partial\Omega} \\ \mathrm{Im}\, f_\mu|_{\partial\Omega} \end{bmatrix} + \begin{bmatrix} \mathrm{Re}\, e^{ikz} \\ \mathrm{Im}\, e^{ikz} \end{bmatrix} = (P_\mu + P_0^k) \begin{bmatrix} \mathrm{Re}\, f_\mu|_{\partial\Omega} \\ \mathrm{Im}\, f_\mu|_{\partial\Omega} \end{bmatrix}.$$

We just need to express the real-linear operators P_μ and P_0^k in block matrix form.

Moreover, the matrix equation is ill-posed, so we use Moore-Penrose pseudoinverse.

Here is one example about writing real-linear operators in block matrix form:

By the properties of the Hilbert transform we get

$$\begin{aligned}\mathcal{P}_\mu(u+iv) &= \frac{1}{2}u+\frac{i}{2}\mathcal{H}_\mu(u)+\frac{1}{2}\mathcal{L}(u),\\ &\quad +\frac{i}{2}v-\frac{1}{2}\mathcal{H}_{-\mu}(v)+\frac{i}{2}\mathcal{L}(v).\end{aligned}$$

Writing real and imaginary parts separately leads to the following block matrix formulation:

$$P_\mu\begin{bmatrix}u\\ v\end{bmatrix}=\frac{1}{2}\begin{bmatrix}u\\ v\end{bmatrix}+\frac{1}{2}\begin{bmatrix}0 & \mathcal{H}_{-\mu}\\ \mathcal{H}_\mu & 0\end{bmatrix}\begin{bmatrix}u\\ v\end{bmatrix}+\frac{1}{2}\begin{bmatrix}\mathcal{L}(u)\\ \mathcal{L}(v)\end{bmatrix}$$

Solution of the boundary integral equation has relative error 0.03% when k=3

Real part

Imaginary part

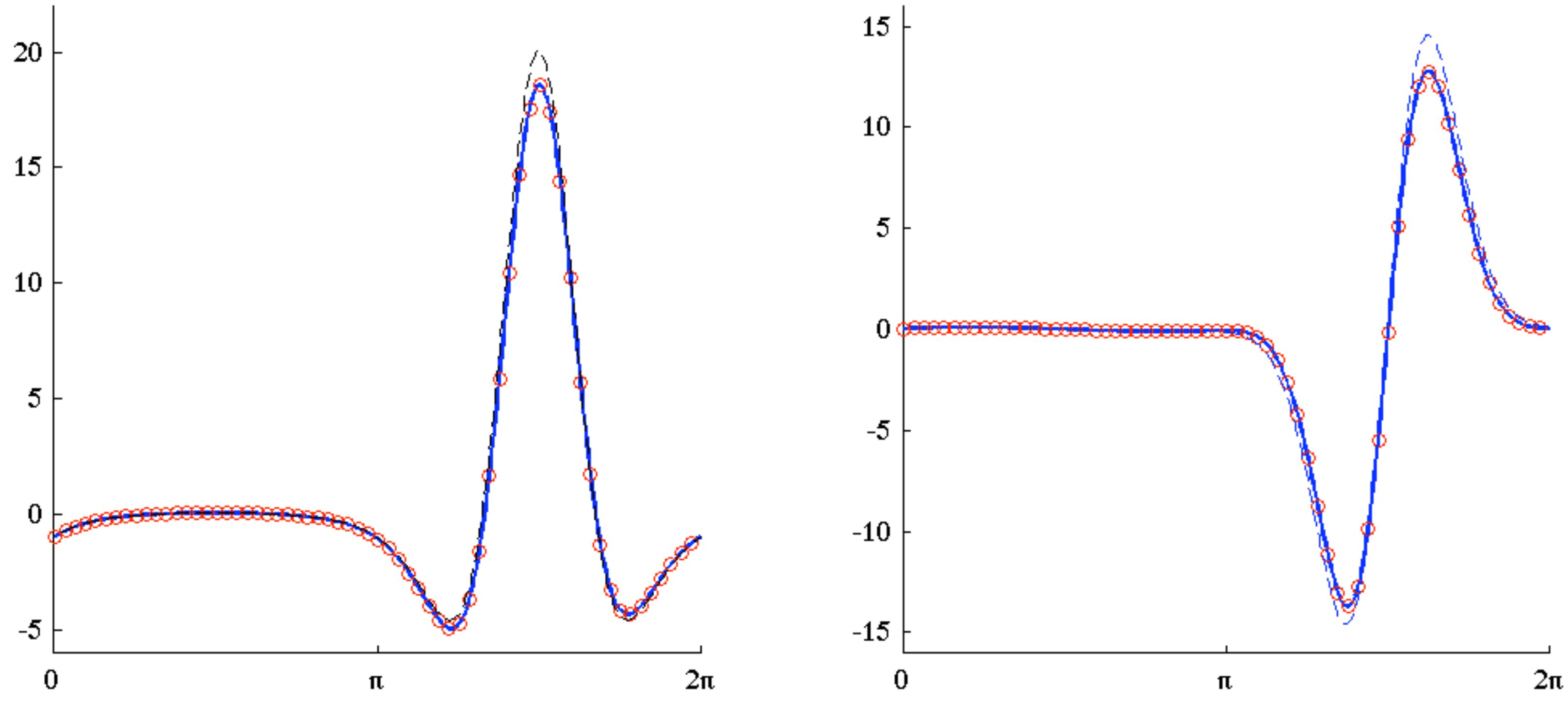

Ground truth ($f_\mu(z,3)|_{\partial\Omega}$)

Calderón exponential ($e^{i3z}|_{\partial\Omega}$)

Solution of the boundary integral equation

Solution of the boundary integral equation has relative error 0.4% when k=5

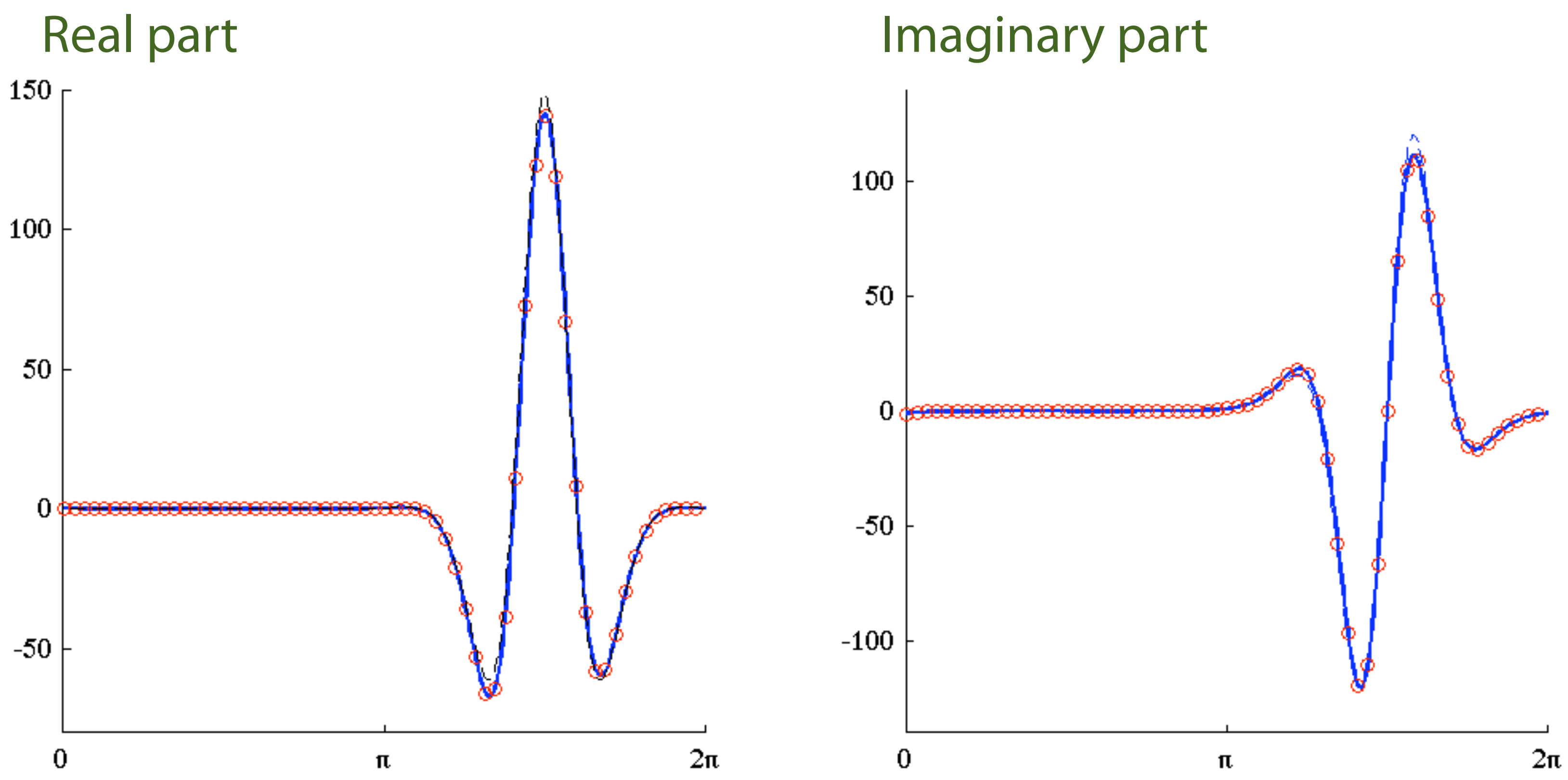

Ground truth ($f_\mu(z,5)|_{\partial\Omega}$)

Calderón exponential ($e^{i5z}|_{\partial\Omega}$)

Solution of the boundary integral equation

Solution of the boundary integral equation has relative error 57% when k=7

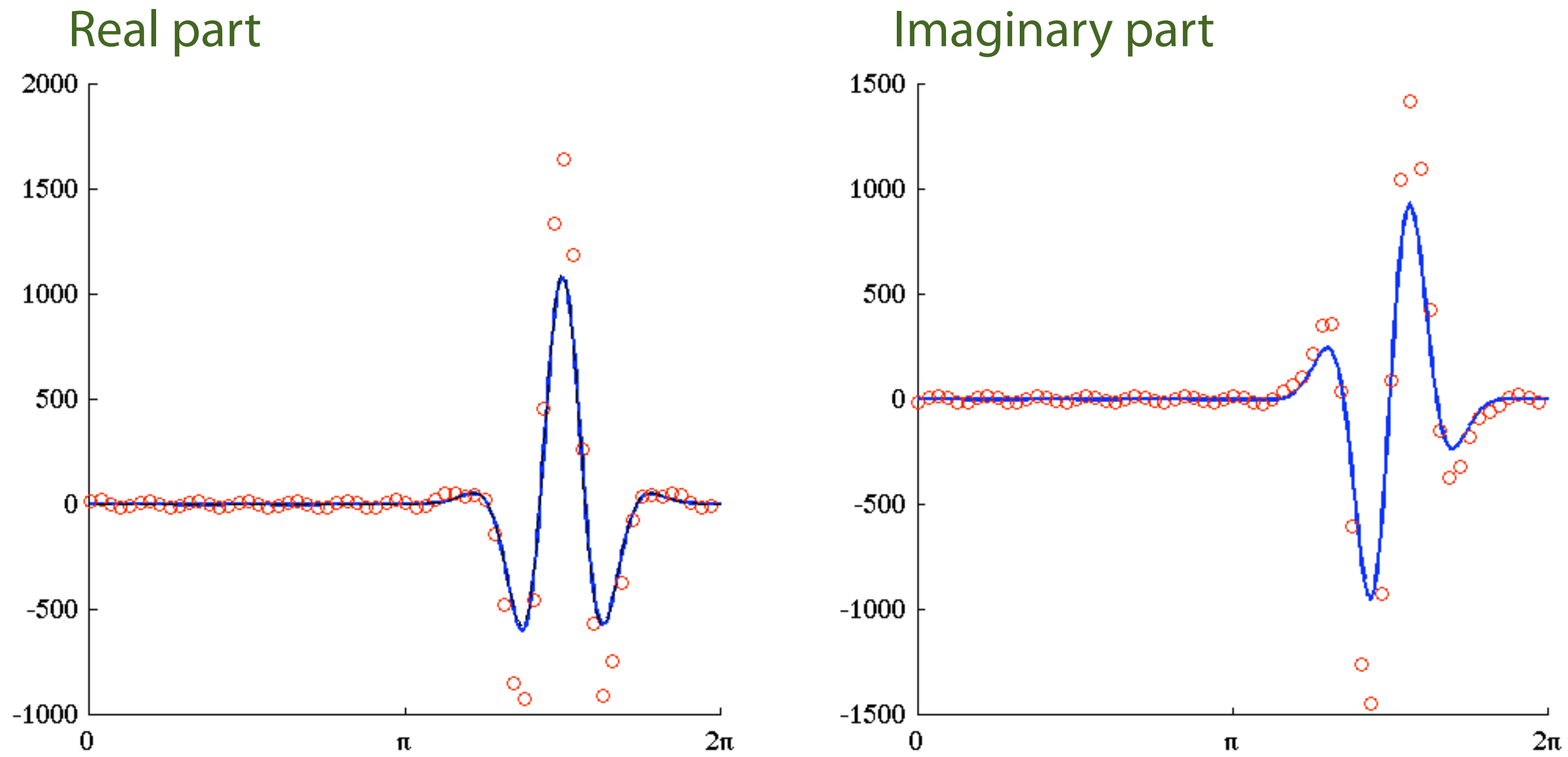

Ground truth ($f_\mu(z,7)|_{\partial\Omega}$)

Calderón exponential ($e^{i7z}|_{\partial\Omega}$)

Solution of the boundary integral equation

Conclusion

Astala and Päivärinta gave the final answer to Calderón's question in dimension two by describing a constructive uniqueness and reconstruction proof.

The aim of this research team (Astala, Mueller, Päivärinta & S) is to design a practical imaging algorithm based on the proof.

The work is partly done: the boundary integral equation can be solved numerically, and it remains to implement solution of the transport matrix equation.

It seems that robustness against noise can be provided by truncating the kernel function in the transport matrix equation.